Burst design and signal processing for the speed of sound measurement of fluids with the pulse-echo technique

Frithjof H. Dubberke, Elmar Baumhögger, and Jadran Vrabec[a)]

Lehrstuhl für Thermodynamik und Energietechnik, Universität Paderborn, Warburger Straße 100, 33098 Paderborn, Germany

(Dated: 19 May 2015)

The pulse-echo technique determines the propagation time of acoustic wave bursts in a fluid over a known propagation distance. It is limited by the signal quality of the received echoes of the acoustic wave bursts, which degrades with decreasing density of the fluid due to acoustic impedance and attenuation effects. Signal sampling is significantly improved in this work by burst design and signal processing such that a wider range of thermodynamic states can be investigated. Applying a Fourier Transformation based digital filter on acoustic wave signals increases their signal-to-noise ratio and enhances their time and amplitude resolutions, improving the overall measurement accuracy. In addition, burst design leads to technical advantages for determining the propagation time due to the associated conditioning of the echo. It is shown that the according operation procedure enlarges the measuring range of the pulse-echo technique for supercritical argon and nitrogen at 300 K down to 5 MPa, where it was limited to around 20 MPa before.

[a)]corresponding author, tel.: +49-5251/60-2421, fax: +49-5251/60-3522, email: jadran.vrabec@upb.de

I. INTRODUCTION

Acoustic measurements allow for a fast and convenient access to the speed of sound, which is a full-fledged thermodynamic property. Such measurements contribute substantially to the development and parameterization of fundamental Helmholtz equations of state (FEOS) for fluids[1], because accurate speed of sound data can efficiently be obtained over a large range of temperature and pressure. The most common measuring principle for determining the speed of sound of liquids is the pulse-echo technique, which was introduced by Kortbeek et al.[2] in 1985. In this method, a burst of sound waves, emitted by an excited quartz crystal, propagates through the fluid over a known distance, is reflected and propagates back to the quartz crystal that also acts as a receiver for the echoes. Two approaches for measuring the propagation time of the wave burst are applied: a) The propagation time of a single wave burst is determined directly[3]. b) The propagation time is determined through cancelation by interference, which takes place at the quartz crystal after emission and reflection of a second wave burst[4,5]. Usually, interference of the echoes is achieved manually by visualizing the resulting wave signals by means of an oscilloscope[4,6].

Both approaches heavily depend on the oscilloscope's sampling resolution of the received wave signals, which limits the accuracy of the time measurement. To increase this accuracy, Ball and Trusler[3] introduced in 2001 a signal analysis that is based on a cross-correlation of the two echoes, which was optimized by a parabolic fit.

Another numerical route for signal enhancement is to apply a Fast Fourier Transformation (FFT) based digital filter to the reflected wave signal. FFT filtering increases the signal-to-noise ratio and reduces offset effects due to hardware and other unwanted side effects[7]. FFT filtering not only enhances the accuracy of the propagation time measurement, and thus the determination of the speed of sound, in combination with numerical analysis it may also simplify the measurement process.

II. MEASUREMENT APPROACHES

The measurement principle of the pulse-echo technique[8,9] is based on a sample cell that has two known propagation path lengths l_1 and l_2, where $l_2 > l_1$. By emitting a modulated high frequency wave burst with a piezoelectric quartz crystal, which is positioned between

two reflectors in the fluid, the speed of sound c is determined by the time measurement of the wave propagation through the fluid, cf. Fig 1. The speed of sound, neglecting dispersion and diffraction effects, is given by the following ratio of propagation distance and time

$$c = \frac{2(l_2 - l_1)}{\Delta t}. \tag{1}$$

Two approaches are used: The single wave burst approach determines the propagation time difference Δt between the two echoes, which is caused by the different propagation path lengths l_1 and l_2, by measuring it directly with a correlation method[3,7]. With the interference approach, as introduced by Kortbeek et al.[2] and later modified by Meier[5], the propagation time difference Δt is measured with the help of an additional second inverse wave burst. Interference occurs between the second echo of the first wave burst and the first echo of the second inverse wave burst, if the second wave burst is emitted with a delay of Δt, cf. Fig. 1. By manually adjusting Δt, the maximum interference can be visually located with an oscilloscope[4,6].

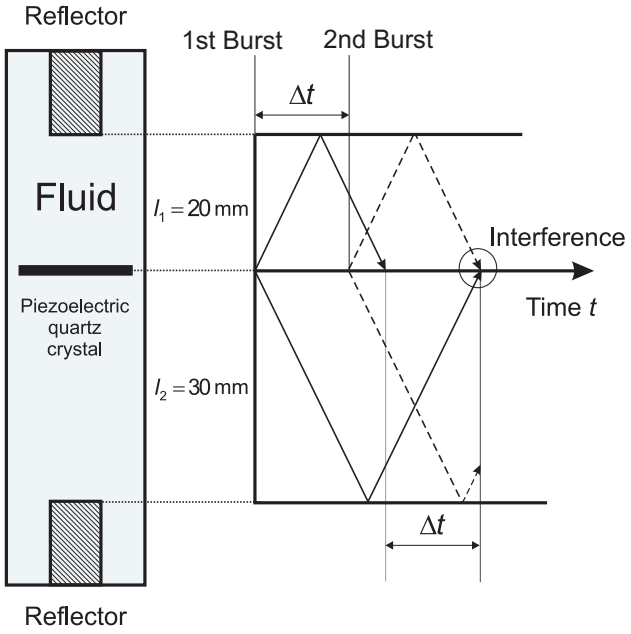

FIG. 1. Principle of the pulse-echo technique for the single wave approach (Δt is the time difference between the received echoes of the wave burst) and interference approach (Δt is the time difference between first and second inverse wave bursts, which cancel out at the quartz due to total interference).

III. SIGNAL ENHANCEMENT

Independent on the measurement approach, determining the speed of sound with a high accuracy requires an undistorted echo signal with a high resolution in time and amplitude as well as low random noise level. To exemplify the associated challenges, the resolution of the oscilloscope employed in the present work (Agilent DSO1022A) in terms of the voltage amplitude was seemingly rather poor at 256 samples (8 bit) compared to its time resolution of 10200 samples (separated by 8 ns). However, at a typical resonance frequency of 8 MHz, this time resolution yields only 15.6 samples per oscillation period and thus affects the uncertainty of the time measurement by about 8 ns. This quantization at low resolution causes a strong distortion of the signal, which is also influenced by random noise.

Applying a FFT based band-pass filter algorithm for signal enhancement is a reliable routine in the present context as shown by Benedetto et al.[7]. It helps to eliminate ambient noise as well as signal distortion and it concurrently increases the resolution of the echo signal. The width of the band-pass filter should be narrow enough to eliminate most of the noise and wide enough to preserve the original signal shape. In this work, a band-pass filter of $\pm$ 20% around 8 MHz (6.4 to 9.6 MHz) was chosen, all other frequency terms were set to zero.

The resolution in time was increased by zero padding in the frequency domain. This was done by appending zero values to the negative and positive end of the Fourier transformed signal data. This did not affect the shape of the signal, but it quadrupled the number of data points by increasing the number of terms in the frequency domain accordingly[10]. Both algorithms were implemented into a data acquisition system and are efficient for interpolating large numbers of data points, increasing the amplitude resolution from 8 bit as provided by the oscilloscope to 64 bit (double) floating-point format with a fourfold resolution in time.

Fig. 2 depicts a section of an increasing echo at low voltage amplitude from the oscilloscope and the same echo reconstructed via FFT with a 6.4 to 9.6 MHz band-pass filter. The quantization of the raw echo signal, noise that randomly causes peaks and the voltage offset are visible. The reconstructed signal has a considerably higher resolution both in terms of amplitude and time, while noise, offset voltage and distortion were significantly reduced.

Fig. 3 (a) displays a raw signal with a high noise ratio as recorded by the oscilloscope. Fig. 3 (b) shows that the absolute value of the frequency spectrum of the signal lies in the

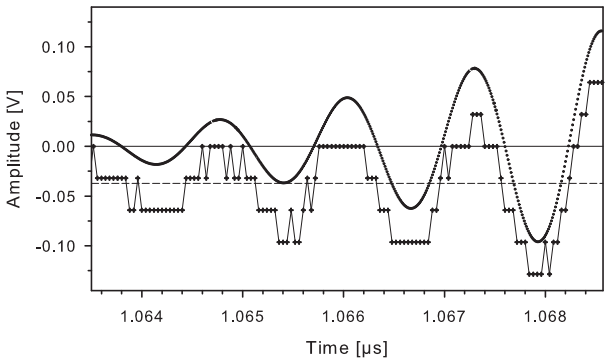

FIG. 2. Detailed view on an echo signal and its FFT reconstructed form. Raw signal (+), reconstructed signal (•), offset voltage (- - -).

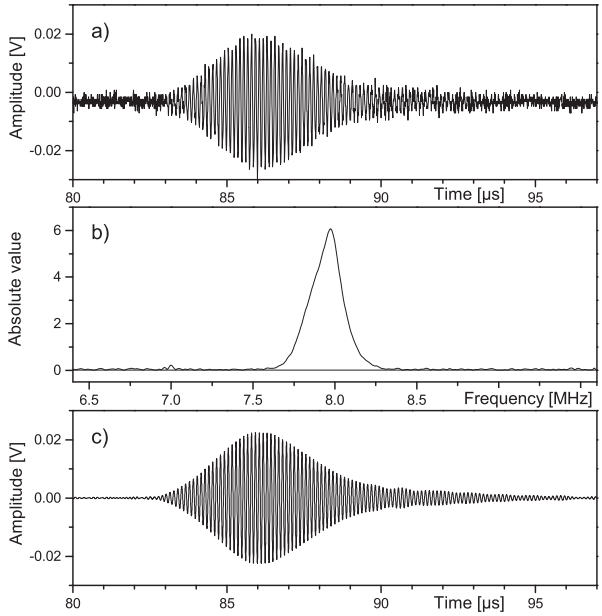

FIG. 3. (a): Raw echo signal with offset voltage, noise and resolution defects due to sampling limits of the oscilloscope; (b): absolute value of the frequency spectrum of the echo signal; (c): echo signal reconstructed by FFT.

range from about 7.6 to 8.3 MHz, which was not affected by the band-pass filter. (Note that a too narrow band-pass filter might cut off crucial properties of the signal.) After transforming the signal back to the time domain, noise and offset voltage were strongly reduced, cf. Fig 3 (c). FFT, band-pass filtering and reconstruction lead to signal data that are much better suited for subsequent numerical operations as discussed in the following.

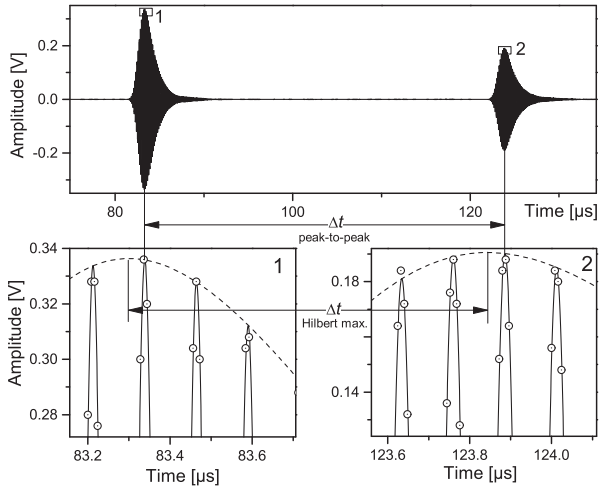

FIG. 4. Top: First (1) and second (2) echo signals as reconstructed by FFT; bottom: magnified view on both echo maxima indicating Δt via peak-to-peak measurement (time between periods with maximum amplitude) and Hilbert transform (time between the envelope maxima); raw echo signal from oscilloscope $\odot$; echo signal reconstructed by FFT ——; Hilbert transform - - -.

IV. TIME MEASUREMENT WITH PEAK-TO-PEAK METHOD AND HILBERT TRANSFORM

For determining the propagation time difference Δt with the single burst approach different methods can be applied, cf. Ball and Trusler[3]. In case of short excitation bursts in dense liquids, which lead to short echoes because of negligible acoustic impedance and attenuation effects, Δt may well be identified as the time between the maximum amplitudes of both echoes, cf. Fig. 4 (top). The maximum amplitudes occur at the equivalent time interval in both echoes[11] and therefore Δt can be derived directly from the timing of the maximum amplitudes. This method was applied here to the minimum and maximum peak and is termed peak-to-peak measurement (PPM) in the following. Fig. 4 (bottom) indicates Δt between the maximum peaks of both echoes with a high resolution. Note that noise inhibits measuring Δt by localizing the start or the end of the two echo waves.

Another method for determining Δt is to evaluate the Hilbert transform (HT) of the echo signals, which may be obtained from basic Fourier analysis and is widely used to map raw periodic functions into analytical signals, that represents the envelope of their varying magnitude[12]. The HT envelope functions yield Δt via their maxima, cf. Fig. 4 (bottom).

Under ideal conditions, where the echoes are perfect, time measurement by single and

double burst methods, PPM and HT should yield throughout the same Δt. However, it was observed in this work that PPM and HT do not necessarily converge to the same Δt under challenging conditions where the fluid density is low, cf. Fig. 4 (bottom). The results from HT seemed to be less reliable, particularly in case of weak signals with a high noise level in combination with a narrow band-pass filter.

V. LIMITATIONS OF PULSE-ECHO APPROACHES

All pulse-echo approaches are limited by the quality of the echoes[12,13], which is influenced by acoustic impedance and attenuation. These effects predominantly play a role in low density fluids, i.e. gases up to the critical region[14] and other highly attenuating liquids[15,16], and impede the readability of the echoes.

The following problems may result: First, the interference approach requires echoes with a plateau shaped amplitude (cf. Fig. 5 (a)), which do not develop in low density fluids. Second, the shape of the echoes becomes so distorted that the interference and correlation approaches do not converge (cf. Fig. 5 (b)). Third, the echoes overlap and interfere due to their increased temporal extension so that they cannot be distinguished anymore (cf. Fig. 5 (c)). Fourth, the echo signal amplitudes decline to zero so that they vanish in the noise.

Fig. 6 illustrates present results from different methods for the speed of sound measurement of gaseous and supercritical nitrogen at 300 K up to a pressure of about 52 MPa compared to the highly accurate FEOS by Span et al.[17]. All experimental results show a decreasing negative trend with respect to the baseline of the FEOS towards low pressure. This is caused by echo distortion, which induces a temporal extension and a shift of the maximum of the echo periods. Uneven echo distortion leads to a larger temporal extension of the second echo, due to its larger propagation distance, than in case of the first echo. Therefore, the correlation method and the PPM sample larger Δt. Echo distortion has a stronger impact on PPM and HT, which depend on the maximum amplitude periods, than on the correlation method, which depends on the entire echo signal. Therefore, measurements below 25 MPa show progressive deviations of up to almost -4 % in case of the correlation method and up to about -8 % and for PPM and HT at 10 MPa. Below 10 MPa, measurements were not feasible here with any pulse-echo method that has been described in the literature, whereas above 25 MPa all methods converged.

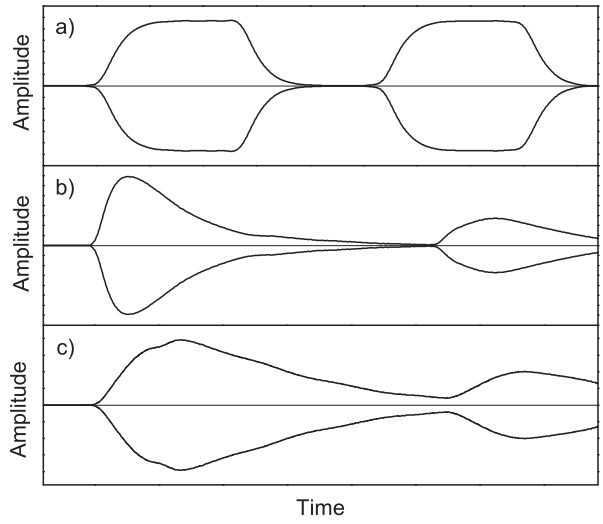

FIG. 5. Limitations of pulse-echo approaches due to acoustic impedance and attenuation illustrated via Hilbert transforms. (a) The interference approach requires echoes with a plateau shaped amplitude as shown here for liquid water at ambient conditions; (b) distorted echoes in nitrogen at 300 K and 10 MPa; (c) distorted and overlapping echoes in nitrogen at 300 K and 7 MPa.

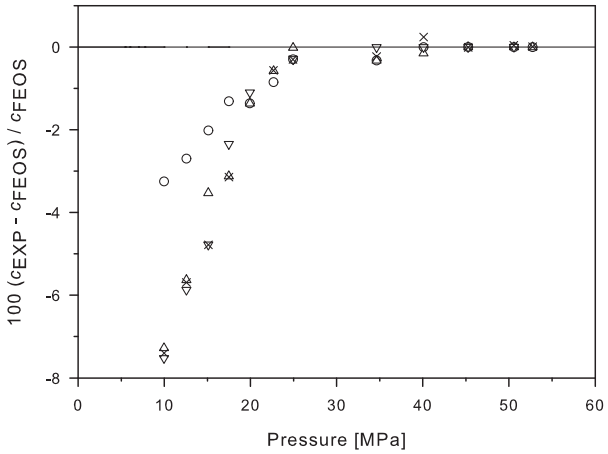

FIG. 6. Speed of sound measurements of nitrogen at 300 K up to a pressure of about 52 MPa for correlation method ($\circ$), peak-to-peak measurement for minimum ($\triangledown$) and maximum ($\triangle$) amplitudes and Hilbert transform ($\times$) compared to the FEOS by Span et al.[17].

VI. PULSE DESIGN

For obtaining echoes with a maximum that is better readable in case of the single burst approach, the burst should be created with only few periods that are modulated by increasing

and decreasing the excitation. Thus, the quartz crystal excitation was modulated here by a sinus burst to which a narrow bandwidth window function (sinus squared) was applied. This has the additional advantage that its narrow-band signal is damping the frequency spectrum such that the distortion of the signal was minimized[18].

In gaseous fluids, the shape of the echoes is less similar to the crystal excitation than in liquid-like fluids. The lower the fluid density, the more burst and echo differ from each other. This is caused by the sustained oscillation of the quartz crystal due to the low acoustic impedance of the fluid, where the kinetic energy of the oscillating quartz crystal is not efficiently transmitted to the fluid. Compared to liquids, gases have a significantly lower acoustic impedance $I_0 = \rho \cdot c$, which quantifies the resistance of the fluid to the propagation of sound[19], mainly due to their low density ρ. Exciting the quartz crystal with fewer periods does not alter the problem of a sustained echo.

Fig. 7 (top) depicts a sinus-modulated burst of 20 periods and the corresponding echo in nitrogen at 300 K and 10 MPa. For better visibility, the echo is plotted with a shifted time axis that matches with the start of the excitation burst. Note that the amplitude axis scales for excitation and echo were chosen according to their different magnitudes. This comparison shows that the echo is much longer than the excitation burst and that it reaches its maximum amplitude with a delay.

In order to prevent a sustained oscillation of the quartz crystal, a brake function was introduced here. The braking was performed by a 180° phase shifted burst immediately following the regular initial burst (20 periods with a peak-to-peak amplitude of 10 V) to which the same sinus squared window function was applied and that was adjustable in its number of periods. Thereby, the oscillation of the quartz crystal was matched to the acoustic impedance that varies for different thermodynamic states of the fluid. To achieve an exact phase shift of the brake function, the excitation frequency was set to the actual resonance frequency of the quartz crystal, which was 7.98 MHz in the present case. Fig. 7 (bottom) shows the resulting echo of an excitation burst with an additional brake function of 17 periods as described above. The echo amplitude has a curved shape that is much better suited for subsequent analysis. It reaches its maximum amplitude approximately at the time of the maximum amplitude of the brake function and it decays much faster than without a brake function.

Fig. 8 shows the shape of both echoes of the excitation bursts illustrated in Fig. 7 with

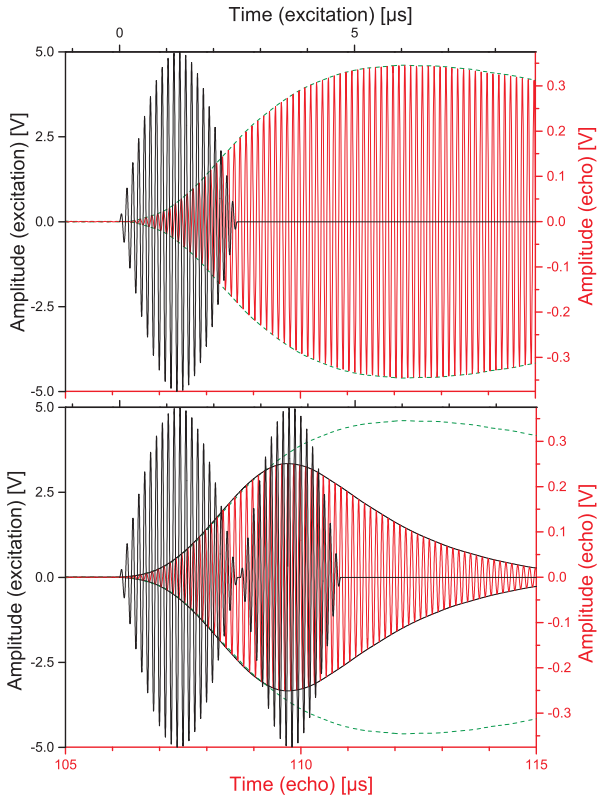

FIG. 7. Excitation burst and echo in nitrogen at 300 K and 10 MPa. Top: Sinusoidal excitation of 20 periods and its echo; bottom: sinusoidal excitation of 20 periods with a brake function of 17 periods and its restrained echo. Dashed lines indicate the Hilbert transform of the echo shown in the upper half of the figure.

and without brake function. For better visibility, only the HT envelopes of the signals were plotted. In case of an excitation burst with 20 periods and a brake function of 17 periods, no peak shift occurred and the maxima were located at period number 30 of both echoes. Without a brake function, the maximum amplitude appears at period number 49 of the first echo and period number 81 of the second echo because of uneven echo distortion. Measuring Δt as the time interval between the peaks in the latter case would thus lead to wrong results.

The sinus-modulated burst with a brake function yields a very distinctive echo due to the narrow peak of its amplitude resulting from the fast decay, locating the period with the maximum amplitude in both echoes at the same position. For echoes from modulated excitations without a brake function this is not the case, cf. Fig. 8.

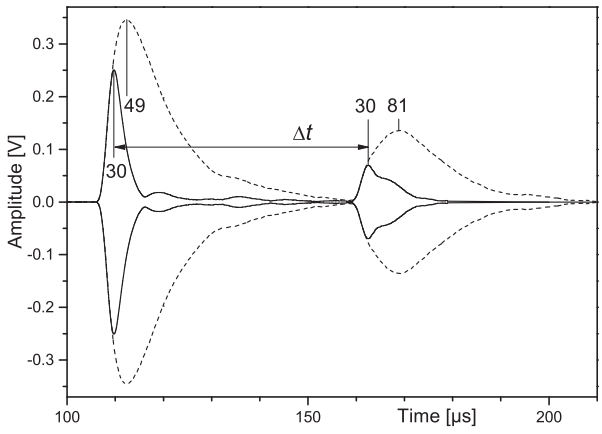

FIG. 8. Hilbert transform of first and second echos in nitrogen at 300 K and 10 MPa. With a break function (——) the position of the maximum amplitude is the same in both echoes; without there is an uneven a peak shift (- - -). The numbers indicate the maximum periods of the echoes.

VII. EXTENSION OF THE MEASUREMENT RANGE FOR GASES

Argon and nitrogen in their gaseous state are well suited as examples for assessing the present method that aims at extending the measurement range of the pulse-echo technique with burst design and signal processing. Due to their importance and availability at high purity (in this work with a given impurity for argon of $\leq$ 10 ppm and for nitrogen of $\leq$ 8 ppm, both purchased at Linde), these fluids have been measured by many authors[20–23].

At around ambient temperature, a minimum pressure for argon of 15 MPa was determined by Meier and Kabelac[6] and of 100 MPa by Kortbeek et al.[2] and for nitrogen of 20 MPa by Meier[5] and Gedanitz[22] for measuring the speed of sound using the pulse-echo technique with the interference approach. These authors were not able to distinguish the echoes below these pressure limits, due to the challenges of the pulse-echo approaches discussed above. Fig. 9 (top) depicts the speed of sound of argon at 300 K up to 52 MPa measured with the correlation method, the PPM for minimum and maximum amplitude and the HT using the brake function in comparison to the FEOS by Tegeler et al.[24]. From 52 MPa down to about 25 MPa all applied methods converge to the baseline of the FEOS. Below 25 MPa, the deviations for measurements carried out with the correlation method increase up to -3.4 % at 5 MPa because of uneven echo distortion. PPM and HT lead to consistent results down to 5 MPa. Below that pressure, measurements were not possible here because of insufficient signal readability.

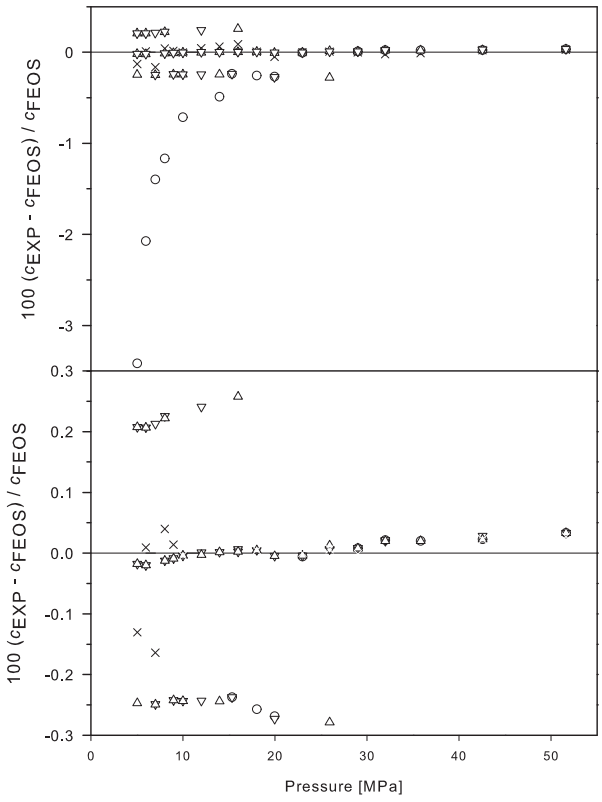

FIG. 9. Top: Speed of sound measurements of argon at 300 K up to a pressure of about 52 MPa with correlation method (○), PPM for minimum (▽) and maximum (△) amplitudes and Hilbert transform (×) with applied brake function; bottom: magnified view of top. The error bars were omitted for better visibility.

For low pressures the PPM lead to a number of measuring points with almost constant offsets. These discrete offsets result from misleading minimum and maximum peak amplitudes with a time difference of $1/(8\ \mathrm{MHz}) = 0.125\ \mu$s due to signal noise and sampling rate of the oscilloscope. This offset increases towards higher pressure, starting at 5 MPa with $\pm 0.2\%$ to almost $\pm 0.3\%$ at 25 MPa due to the ratio of propagation distance and time, cf. Fig. 9 (bottom) and Eq. (1). In contrast to the PPM, the HT method does not depend on discrete periods for Δt measurements and responds to signal noise by scattering results for pressures below 30 MPa. Fig. 9 (bottom) is a magnified view on Fig. 9 (top) and depicts the results from PPM for minimum and maximum amplitudes and HT in a deviation range of ± 0.1 % over the pressure.

The present measurements were carried out with an apparatus based on the pulse-echo

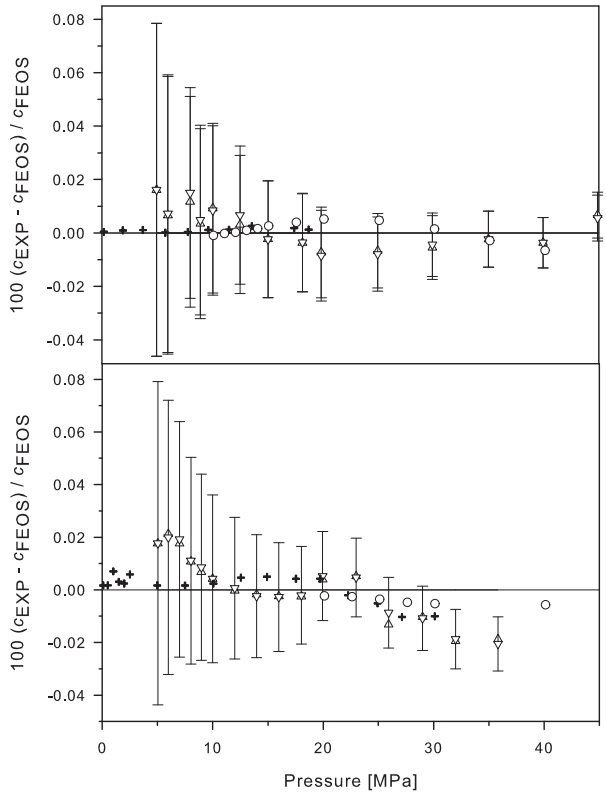

FIG. 10. Top: Speed of sound measurements of argon at 350 K up to a pressure of about 45 MPa with PPM for minimum ($\triangledown$) and maximum ($\triangle$) amplitudes, Estrada-Alexanders and Trusler[23] (+), Meier and Kabelac[6] ($\circ$) compared to the FEOS by Tegeler et al.[24]; bottom: Speed of sound measurements of nitrogen at 300 K up to a pressure of about 36 MPa for PPM for minimum ($\triangledown$) and maximum ($\triangle$) amplitudes, Costa-Gomez et al.[20] (+), Meier[5] ($\circ$) compared to the FEOS by Span et al.[17].

technique with double path length as presented recently[9]. The overall uncertainties of up to $\pm 0.06\%$ are mainly due to the uncertainty of the pressure (± 100 Pa) and temperature (± 15 mK) measurement. The uncertainty of pressure measurement alone is responsible for almost up to ± 0.05 % of the uncertainty, cf. Fig. 10. The overall uncertainty, however, is within the experimental error. With an increasing temporal extension of the echo due to distortion, as seen for low density fluids, the determination of the speed of sound may be offset due to the ambiguity of the maximum period, cf. Fig. 9. This problem affects the interference approach and the correlation method as well. Therefore, measurements should be carried out starting from a high density, where results are unambiguous, going down to

low density state points step by step.

VIII. CONCLUSION

It was shown that the direct time difference measurement approach with burst design and signal processing, either based on PPM or on the HT, has advantages over the traditional correlation method as well as the interference method for fluids in gaseous and supercritical states. The present results show that speed of sound measurements for argon and nitrogen are feasible with the pulse-echo technique down to a pressure of 5 MPa at ambient temperature. Hence, the new procedure extends the measurement range of the pulse-echo technique so that it better overlaps with that of other speed of sound measurement techniques. E.g., argon was measured by Estrada-Alexanders and Trusler[23] in a spherical resonator up to a pressure of 19 MPa.

IX. ACKNOWLEGDEMENTS

The authors thank Bernd Henning, Fabian Bause, Jens Rautenberg and Andreas Schröder from the Chair of Measurement and Engineering at the University of Paderborn for fruitful discussions and their support.

REFERENCES

[1]R. Span, *Multiparameter Equations of State: An accurate source of thermodynamic property data* (Springer, Berlin, 2000).

[2]P. Kortbeek, M. Muringer, N. Trappeniers, and S. Biswas, Rev. Sci. Instrum. **56**, 1269 (1985).

[3]S. Ball and J. Trusler, Int. J. Thermophys. **22**, 427 (2001).

[4]H. Gedanitz, M. Davila, E. Baumhögger, and R. Span, J. Chem. Thermodyn. **42**, 478 (2010).

[5]K. Meier, *The Pulse-echo Method for High Precision Measurements of the Speed of Sound in Fluids* (Habilitation Thesis, University of the Federal Armed Forces, Hamburg, 2006).

[6]K. Meier and S. Kabelac, Rev. Sci. Instrum. **77**, 123903 (2006).

[7]G. Benedetto, R. Gavioso, P. G. Albo, S. Lago, D. M. Ripa, and R. Spagnolo, Int. J. Thermophys. **26**, 1667 (2005).

[8]C. Lin and J. Trusler, J. Chem. Phys. **136**, 094511 (2012).

[9]F. H. Dubberke, D. B. Rasche, E. Baumhögger, and J. Vrabec, Rev. Sci. Instrum. **85**, 084901 (2014).

[10]J. Borkowski and J. Mroczka, Measurement **43**, 1595 (2010).

[11]S. J. Orfanidis, *Electromagnetic Waves and Antennas* (Rutgers University, Piscataway, NJ, 2014).

[12]S. Sugasawa, Jpn. J. Appl. Phys. **41**, 3299 (2002).

[13]P. L. Edwards, J. Acoust. Soc. Am. **73**, 1608 (1983).

[14]R. Gordon, Physica **34**, 398 (1967).

[15]K. Matsuzawa, N. Inoue, and T. Hasegawa, J. Acoust. Soc. Am. **81**, 947 (1987).

[16]J. Champion, C. Langton, G. Meeten, and N. Sherman, Meas. Sci. Technol. **1**, 786 (1990).

[17]R. Span, E. W. Lemmon, R. T. Jacobsen, W. Wagner, and A. Yokozeki, J. Phys. Chem. Ref. Data **29**, 1361 (2000).

[18]F. J. Harris, Proc. IEEE **66**, 51 (1978).

[19]B. Henning and J. Rautenberg, Ultrasonics **44**, 1395 (2006).

[20]M. C. Gomez and J. Trusler, J. Chem. Thermodyn. **30**, 527 (1998).

[21]P. Kortbeek, N. Trappeniers, and S. Biswas, Int. J. Thermophys. **9**, 103 (1988).

[22]H. Gedanitz, *Schallgeschwindigkeits- und Dichtemessungen in Fluiden* (PhD thesis, Ruhr-University Bochum, 2010).

[23]A. F. Estrada-Alexanders and J. P. M. Trusler, J. Chem. Thermodyn. **27**, 1075 (1995).

[24]C. Tegeler, R. Span, and W. Wagner, J. Phys. Chem. Ref. Data **28**, 779 (1999).